Int. J. Multiphase Flow Vol. 15, No. 6, pp. 877–892, 1989
Printed in Great Britain.

0301-9322/89 $3.00 + 0.00

EFFECT OF LIQUID VISCOSITY ON THE STRATIFIED–SLUG TRANSITION IN HORIZONTAL PIPE FLOW

N. ANDRITSOS
Chemical Process Engineering Research Institute, P.O. Box 19517, 540 06 Thessaloniki, Greece

L. WILLIAMS and T. J. HANRATTY
Department of Chemical Engineering, University of Illinois, Urbana, IL 61801, U.S.A.

(*Received* 21 *March* 1988; *in revised form* 27 *December* 1988)

Abstract—The effect of liquid viscosity on the initiation of slug flow was studied in horizontal 2.52 and 9.53 cm pipelines. The results show the stabilizing effect of viscosity predicted by Lin & Hanratty, and are at variance with analyses which use a long-wavelength inviscid approximation. For very viscous liquids a stability analysis which recognizes that slugs originate from a train of small-wavelength sinusoidal waves seems consistent with the measurements.

Key Words: two-phase flow, horizontal, gas–liquid, transition, slug flow, experimental, liquid viscosity

INTRODUCTION

This paper presents the results of experiments on the effect of liquid viscosity on the transition from a stratified pattern to a slug pattern for gas–liquid flow in a horizontal pipeline. They suggest a new mechanism, whereby the precursor to slug formation is the appearance of small-wavelength Kelvin–Helmholtz (KH) waves. This mechanism is applicable to liquids with viscosities >20 cP, and could be important in large diameter pipelines.

The transition from a stratified pattern to a slug pattern for a horizontal gas–liquid flow has been the subject of a number of theoretical studies. Early works by Kordyban & Ranov (1970) and Wallis & Dobson (1973) explored a stability mechanism, whereby the slugs arise from the growth of infinitesimal disturbances at the interface. Since the spacing between the slugs is large compared to the pipe diameter it was natural to restrict the analysis to waves which have a large wavelength compared to the height of the gas space. If viscous effects are neglected the following condition for instability is obtained for a horizontal rectangular channel of height B:

$$k\rho_L(u - C)^2 \coth kh_L + k\rho_G(U - C)^2 \coth kh_G = g(\rho_L - \rho_G) + \sigma k^2, \quad [1]$$

where k is the wavenumber, U is the gas velocity, u is the liquid velocity, h_G is the height of the gas space, h_L is the height of the liquid space, ρ_G is the gas density, ρ_L is the liquid density and g is the acceleration of gravity. For large waves ($kh_L \ll 1$, $kh_G \ll 1$) and for negligible surface tension effects the following instability condition is obtained from [1]:

$$\frac{U^2}{gh_G}\frac{\rho_G}{\rho_L}\left(\frac{C}{U} - 1\right)^2 > \frac{(\rho_L - \rho_G)}{\rho_L} - \frac{u^2}{gh_L}\left(\frac{C}{u} - 1\right)^2; \quad [2]$$

and the wave velocity, C, is

$$C = \frac{U\rho_G h_L + u\rho_L h_G}{\rho_L h_G + h_L \rho_G}. \quad [3]$$

If $\rho_G h_L/\rho_L h_G$ is small compared to unity [2] and [3] simplify to

$$(U - u) > \left[\frac{g(\rho_L - \rho_G)h_G}{\rho_G}\right]^{1/2} \quad [4]$$

and

$$C = u + U\frac{\rho_G h_L}{\rho_L h_G}. \quad [5]$$

The physical interpretation of the KH instability represented by [4] is as follows: the presence of waves at the interface causes a velocity maximum in the gas at the crest and a velocity minimum at the trough. According to the Bernoulli equation this flow variation is associated with a pressure minimum at the liquid surface at the crest and a pressure maximum at the trough. If the destabilizing influence of these forces is large enough to overcome the stabilizing effect of gravity, instability occurs.

Wallis & Dobson (1973) performed transition studies in rectangular channels and concluded that [4] overpredicts the critical gas velocity by a factor of about two. A number of authors have argued that this discrepancy can be explained by considering non-linear effects. The analyses of Kordyban (1977), Mishima & Ishii (1980) and Wallis & Dobson (1973) suggest a criterion of the same form as [4] with factors of 0.74, 0.49 and 0.50 on the r.h.s. Taitel & Dukler (1976) suggest that instability occurs in a channel when

$$(U-u) > \left(1-\frac{h_L}{B}\right)\left[\frac{g(\rho_L-\rho_G)h_G}{\rho_G}\right]^{1/2}. \qquad [6]$$

For gas–liquid flow in a pipe they give

$$U > \left(1-\frac{h_L}{D}\right)\left[\frac{g(\rho_L-\rho_G)A_G}{\rho_G S_i}\right]^{1/2}. \qquad [7]$$

Here S_i is the length of the interface

$$\frac{S_i}{D} = \left[1-\left(2\frac{h_L}{D}-1\right)^2\right]^{1/2}, \qquad [8]$$

h_L is the height measured from the bottom of the pipe, D is the diameter and A_G is the area occupied by the gas.

Recently, Lin & Hanratty (1986), Hanratty (1987) and Wu et al. (1987) have re-examined the possibility of explaining the transition from stratified to intermittent flow by linear stability theory. They retained the assumption that the wavelength is long compared to h_G, or h_L, but abandoned the assumption of inviscid flow by including the effects of the drag of the gas on the liquid, τ_i, and of the resisting stress of the wall on the liquid, τ_{WL}. Equation [2] still holds provided the velocity profiles in the liquid and the gas can be approximated by plug flows. The principal differences found by Lin & Hanratty is that the wave velocity is not given by [3] or [5].

The first term on the l.h.s. of [1] represents the destabilizing effect of liquid inertia. For air–water flows, $\rho_G/\rho_L = 1.2 \times 10^{-3}$ and [5] simplifies to $C = u$ for the range of conditions over which the transition is observed. Consequently, the inviscid KH analysis predicts no influence of liquid inertia on neutral stability since it predicts $(C/u - 1) \cong 0$. It represents a static instability. In contrast, the viscous analysis of Lin & Hanratty gives non-zero values of $(C/u - 1)$ because of the inclusion of the effects of τ_i and τ_w. As a result, an important destabilizing effect of liquid inertia is predicted by the long-wavelength viscous KH analysis for low viscosity liquids. The inclusion of viscous stresses, therefore, gives the surprising effect of causing the air–water system to be more unstable, in that the initiation of long-wavelength interfacial disturbances is predicted to occur at much lower gas velocities (consistent with experimental observation) that is given by an inviscid KH analysis. The theoretical significance is that a mechanism for the initiation of intermittent flow by the growth of infinitesimal disturbances cannot be ruled out.

These theoretical results of Lin & Hanratty (1986) are illustrated in figure 1. The system being considered is a concurrent flow of gas and liquid in a horizontal rectangular channel of height B. The ordinate is the dimensionless liquid height, h_L/B. The dashed curve is the superficial gas velocity, U_{SG}, predicted by an inviscid analysis for the growth of long-wavelength disturbances. The solid curves are the viscous predictions for air–water flow. In this case the interface is covered by small-wavelength waves when intermittent flow is initiated. Therefore, the analysis envisions a long-wavelength disturbance superimposed upon the roughened interface. The effect of these waves is felt by an increase in the interfacial stress. The parameter f_i/f_s is the ratio of the friction factor

$$f_i = \frac{\tau_i}{\frac{1}{2}\rho U^2} \qquad [9]$$

to the friction factor for a smooth wall, f_s. A transition at lower gas velocities predicted by the viscous analysis is clearly indicated.

Lin & Hanratty (1986) also present stability calculations for liquids other than water. The predicted effect of an increase in liquid viscosity, when presented in a plot such as figure 1, is to translate the solid curves upward. The viscous analysis thus predicts a stabilization with increasing viscosity (when viewed in this type of plot). However, the reason for this is not because of the increased damping of disturbances. Since comparisons are made at fixed h_L/B, increases in viscosity are accompanied by decreases in the liquid flow rate for a given U_{SG}. The inertia of the liquid and, therefore, its destablilizing effect decreases with increasing liquid viscosity. For sufficiently high liquid viscosity, destabilizing effects of liquid inertia become negligible and the Lin & Hanratty analysis is represented by the dashed curve. It, therefore, gives the surprising result that the inviscid theory becomes more accurate as the liquid viscosity increases.

When the Lin & Hanratty analysis is exhibited in Mandhane coordinates (U_{SL} vs U_{SG}), rather than in the coordinates used in figure 1, the interpretation becomes more complicated. An increase in liquid viscosity has two opposing effects: for a fixed U_{SG}, an increase in the liquid viscosity will be associated with the destabilizing effect of an increase in h_L for any given U_{SL}. However, an increase in viscosity is accompanied by a smaller U_{SL} for any h_L. This decreases the destabilizing effect of liquid inertia.

Lin & Hanratty (1986) tested their analysis by carrying out laboratory studies of air and water flowing in a 2.52 cm i.d. pipe with a length of 600 pipe diameters and in a 9.53 cm i.d. pipe with a length of 260 pipe diameters. They found that for $U_{SG} > 3.3$ m/s the slugs were formed by a nonlinear mechanism involving the coalescence of large-amplitude irregular waves. Consequently, it could be expected that a transition caused by the growth of infinitesimal disturbances could be applicable only for $U_{SG} < 3.3$ m/s. A comparison of the transition for air–water observed under this restriction agrees quite well with predictions based on the viscous, long-wavelength KH analysis if f_i/f_s is taken equal to 2, a reasonable assumption for air–water flow in this range of h_L/D (Andritsos & Hanratty 1987b).

However, these tests with air and water are also in approximate agreement with the non-linear analyses discussed above. This pointed out the need for additional experiments and prompted the initiation of a laboratory study of the effects of changes of the liquid viscosity. The results of this effort are presented in this paper. The strong effect of liquid viscosity predicted by Lin & Hanratty, when the transition data are plotted as h_L/D vs U_{SG}, is observed. However, a closer comparison shows differences between laboratory observations and the Lin & Hanratty analysis. This prompted additional detailed studies of the mechanisms for the initiation of slugs. On the basis of these tests

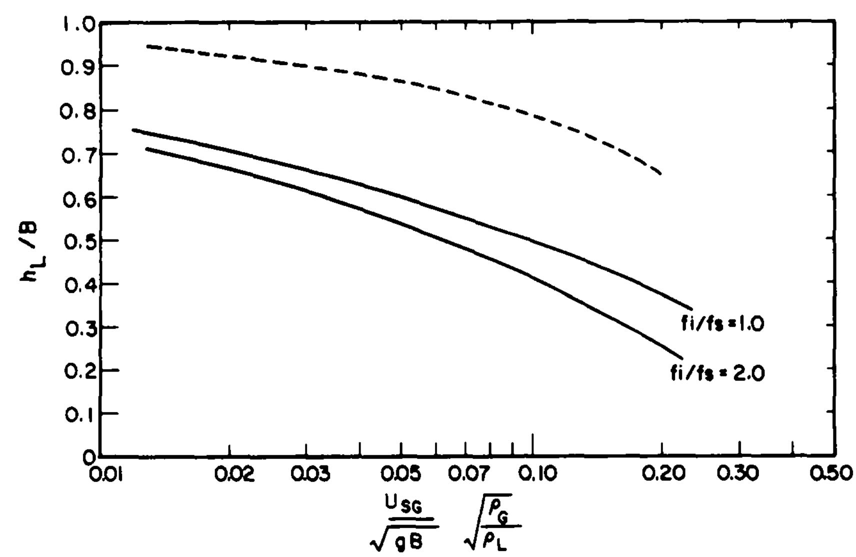

Figure 1. Stability analysis for stratified flow in a channel of height B: – – –, inviscid KH analysis; ——, viscous KH analysis. $\rho_G/\rho_L = 1.12 \times 10^{-3}$, $\nu_G/\nu_L = 16.1$.

it is argued that a KH stability analysis can be used for high viscosity liquids only if the assumption of long-wavelength disturbances is abandoned.

An important ingredient in developing these arguments is the recent study by Andritsos & Hanratty (1987a), over a range of liquid viscosities of 1–80 cP, of the initiation of waves in stratified gas–liquid flows. For air and water the first waves observed with increasing gas velocity are generated by a sheltering mechanism involving pressure variations in phase with the wave slope. At larger gas velocities irregular, large-amplitude waves appear. These are initiated by gas-phase pressure variations 180° out of phase with the wave height (a KH mechanism). The influence of pressure variations in-phase with the wave slope becomes less important with increasing liquid viscosity. In fact, at sufficiently high liquid viscosities the first waves that appear with increasing liquid viscosity are the KH waves.

This influence of liquid viscosity has been pointed out some years earlier by Francis (1954, 1956) and Miles (1959). Both Francis and Andritsos & Hanratty observed the same mechanism for the initiation of waves on a very viscous liquid. The first disturbances observed with increasing gas velocity are small-amplitude, small-wavelength, rather regular 2-D waves. With a slight increase in gas velocity, these give way to a few large-amplitude waves with steep fronts and smooth troughs, and with spacings that can vary from a few centimeters to a meter. Ocassionally, several small 2-D waves can be seen in front of the large waves.

In this paper evidence will be presented that events leading to the appearance of intermittent flow at low gas velocities or to the appearance of large-amplitude irregular waves at large gas velocities are the same. Consequently, an attempt will be made to interpret both phenomena by the same stability analysis. Similar approaches have been adopted previously by Wallis & Dobson (1973) and by Andreussi & Persen (1987). The large-amplitude waves seem to have been given a number of names: slugs by Wallis & Dobson (1973); roll waves, by Lin (1985); large disturbance waves, by Andreussi & Persen (1984); and irregular large-amplitude waves, by Andritsos (1986). Since the initiation of these waves has been shown by Miles (1959) and by Andritsos & Hanratty (1987a) to be due to a Kelvin–Helmholtz instability it seems appropriate to call them Kelvin–Helmholtz (KH) waves.

DESCRIPTION OF THE EXPERIMENTS

The experimental results, discussed in this paper, for the 10 m horizontal 2.52 cm pipe are from the studies of Andritsos & Hanratty (1987a) for the flow of air and liquids with viscosities of 1, 4.5, 16 and 70 cP. The results for 25 m horizontal 9.53 cm pipeline were obtained recently in a new facility constructed by L. Williams. Transitions were observed with glycerine–water solutions having viscosities of 1, 20 and 100 cP. Simple T-junction entries were used for mixing the two phases at the inlet in both studies. In the 9.53 cm pipe the gas and liquid were introduced at two different locations.

The thickness of the liquid layer flowing along the bottom of the pipe, h_L, was measured in one test section by two parallel-wire conductance probes which extended vertically across the whole pipe cross section. For experiments in which small-wavelength waves were present the liquid height was represented as the time-average of the signal from the conductance probes. A second test section used pairs of short parallel 0.51 mm chromel wires at 45° intervals to measure the variation of the liquid height around the pipe circumference. In the 2.52 cm pipe the two sections were separated by 10.2 cm, and in the 9.23 cm pipe, by 26.7 cm.

EXPERIMENTAL RESULTS

(a) Mandhane plots

A map of the different flow regimes observed in the 2.52 cm pipe is given in figure 2. The solid line is for a liquid of 4.5 cP; the dashed line for 1.0 cP. Both shown a large region where the pseudo-slugs, described by Lin & Hanratty (1987a), occur. These are large-amplitude waves which touch the top wall. They differ from slugs in that they are not accompanied by large pressure fluctuations and they can lose their coherency as they move down the pipe.

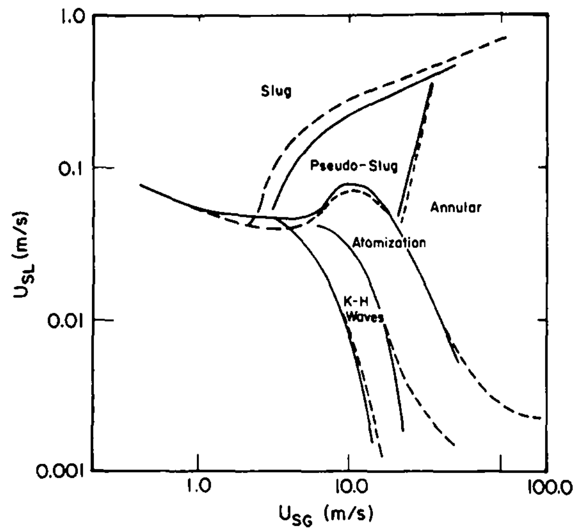

Figure 2. Flow regimes for the 2.52 cm horizontal pipe: ——, 4 cP liquid; – – –, 1 cP liquid. The transition to regular small-amplitude waves is not shown.

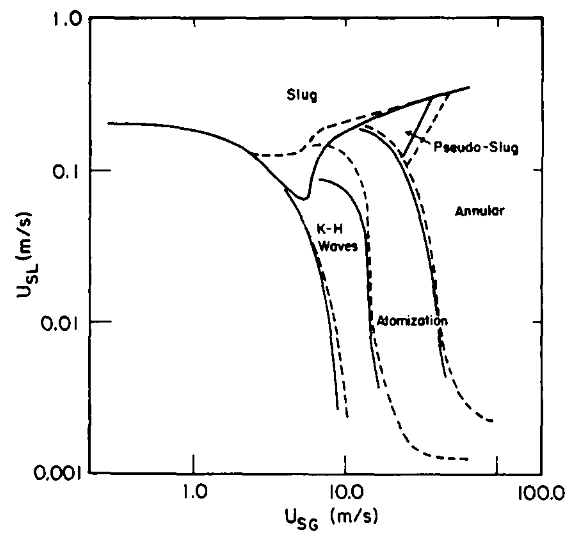

Figure 3. Flow regimes for a 20 cP (——) and a 1 cP (– – –) liquid in the 9.53 cm horizontal pipe. The transition to regular small-amplitude waves is not shown.

As discussed by Andritsos & Hanratty (1987a), the first waves that appear on a stratified flow with increasing gas velocity are small-amplitude, regular 2-D waves associated with gas-phase pressure variations in phase with the wave slope. This transition is not shown. At larger gas velocities large-amplitude irregular waves appear that are associated with pressure variations in phase with the wave height (KH waves).

Andritsos & Hanratty (1987a) give results similar to those shown in figure 2 for 16 and 70 cP liquids. These show a decrease in the liquid velocity required to initiate slug flow at low gas velocities. For the 16 cP liquid the regular waves appear over a very narrow range of gas velocities and for the 70 cP liquid they do not appear at all.

Observed transitions in the 9.53 cm pipe are shown in figures 3 and 4 for 20 and 100 cP liquids. It is noted that the pseudo-slug region decreases in size with increasing pipe diameter and increasing liquid viscosity. In fact, it is not observed for the 100 cP liquid in the 9.53 cm pipe.

The behavior at the transition to slug flow can be separated into three regions (which are most evident for the high viscosity liquids). The first is for gas velocities which are too low for the appearance of KH waves in a stratified flow ($U_{SG} < 4$ m/s). The second extends to the gas velocity at which pseudo-slugs first appear in the 9.53 cm pipe ($U_{SG} = 4 - 12$ m/s). The third is for $U_{SG} > 12$ m/s.

For most of the first regime the flow is not fully-developed and the liquid flow is greatly influenced by the hydraulic gradient that exists along the entire pipe, even though its length is 400 pipe diameters for the 2.52 cm pipe and 260 pipe diameters for the 9.53 cm pipe. When such hydraulic gradients exist the liquid flowing for a given h_L/D is larger since it is being moved both by the gas drag at the interface and the hydraulic gradient. Because the initiation of slugs is primarily dependent on h_L/D, the U_{SL} values corresponding to slug flow transitions at low U_{SG} in figures 2–4 are higher than would be observed for a fully-developed flow. This effect increased with increasing liquid viscosity, increasing pipe diameter and decreasing liquid velocity. This non-developed condition was observed for low liquid viscosities at $U_{SG} < 2$ m/s in the 2.52 cm pipe and at $U_{SG} < 3.5$ m/s in the 9.53 cm pipe. It was observed for a liquid with a viscosity of 100 cP at $U_{SG} < 4.5$ m/s in the 9.53 cm pipe. Figure 5 illustrates this effect for air–water flow in the 9.53 cm pipe. Here it is noted that at low gas velocities the height of the liquid is insensitive to changes in U_{GS} and depends only on the location in the pipe.

The appearance of KH waves in a stratified flow is accompanied by a large increase in the interfacial stress and a drastic thinning of the liquid layer, as illustrated in figure 6. Because of this thinning of the liquid much larger U_{SL} are required to initiate slugs. This is reflected by the sharp rise in the transition curve for $U_{SG} = 4.5 - 12$ m/s in figure 4 for a 100 cP liquid. The transition to slug flow observed with increasing liquid flow in this region in the 9.53 cm pipe for all liquids

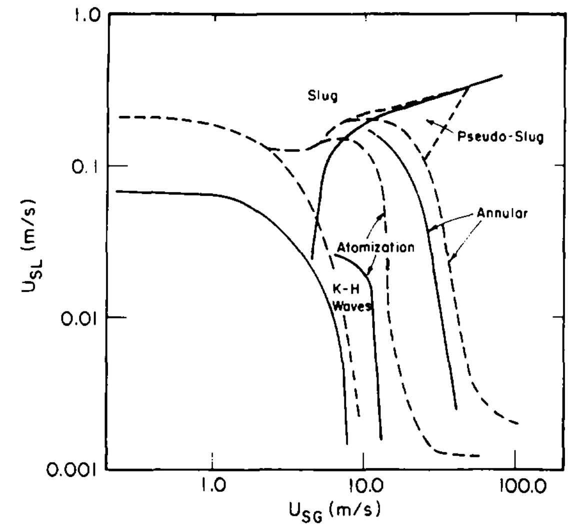

Figure 4. Flow regimes for a 100 cP (——) and a 1 cP (- - -) liquid in the 9.53 cm horizontal pipe.

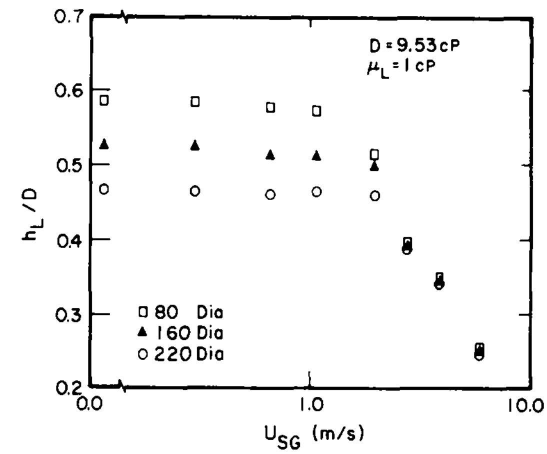

Figure 5. Plot showing that at low gas velocities the height of the liquid is insensitive to changes in gas velocity and is mainly dependent on the location in the pipe.

and in the 2.52 cm pipe for 16 and 70 cP liquids is very sharp and accompanied by large pressure pulsations. For the lower viscosity liquids in the 2.52 cm pipe the existence of a large pseudo-slug region makes the definition of the transition more difficult.

The transition to slug flow with increasing liquid velocity at $U_{SG} > 12$ m/s is harder to define because of the presence of pseudo-slugs. Slugs move approximately with the gas velocity. At transition only one slug will exist in the pipeline. After its passage the liquid level in the pipe is greatly reduced. Pseudo-slugs, that are present between the appearance of slugs, travel at velocities up to 30% of the gas velocity and carry liquid with them. Consequently, it may take as much as 5 min after the passage of a slug for the liquid to thicken enough for another slug to appear. The presence of a slug was detected from measurements of pressure fluctuations, as discussed by Lin & Hanratty (1987b). It is noted from figures 2–5 and from figures 13 and 14 in the paper by Andritsos & Hanratty (1987a) that the transition curve in a Mandhane plot at $U_{SG} > 12$ m/s is approximately independent of liquid vicosity and of pipe diameter for pipe sizes from 2.54 to 9.53 cm.

(b) Effect of liquid height on transitions

In order to obtain a mechanistic understanding of the transition to slug flow, it is useful to plot the ratio of the liquid height and the pipe diameter, h_L/D, vs superficial gas velocity, U_{SG}. This type of plot may also have the advantage that it is less sensitive to whether the flow is underdeveloped.

Figure 7 presents results obtained in the 9.53 cm pipe. The h_L were measured just prior to transition at locations in the pipe where slugs were first observed. Transitions were observed at the middle of the pipe for liquids with viscosities <20 cP and upstream of the middle for large liquid viscosities. In some cases the gas velocity at which the liquid height was measured was 20% smaller than that required to initiate slugs. Therefore, the values of h_L may be somewhat higher than the true values.

The open symbols in figure 7 represent conditions where a transition to slug flow was observed. The solid symbols represent conditions where a transition to KH waves was observed. Consider the results for a 100 cP liquid. It is seen that for $U_{SG} <$ ca. 5 m/s and $h_L/D >$ ca. 0.4 that the h_L/D required for the appearance of roll waves varies strongly with U_{SG}. For these conditions the interface is smooth at the transition to slugging. However, for $U_{SG} >$ ca. 5 m/s the interface of the 100 cP liquid is roughened with large-amplitude waves when slugs appear. For the range of gas velocities of 5–9 m/s the h_L/D at transition is approximately constant and equal to 0.4. At $U_{SG} >$ ca. 9 m/s the h_L/D again decreases with increasing U_{SG}. For $h_L/D <$ ca. 0.4 the first transition with a 100 cP liquid that is observed is the initiation of large-amplitude waves. For example, for

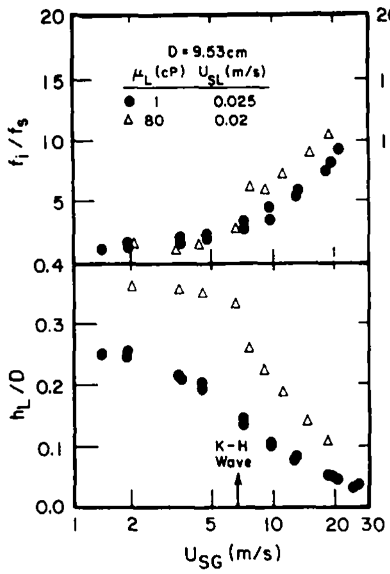

Figure 6. Effect of the appearance of KH waves on the height of the liquid and the interfacial drag.

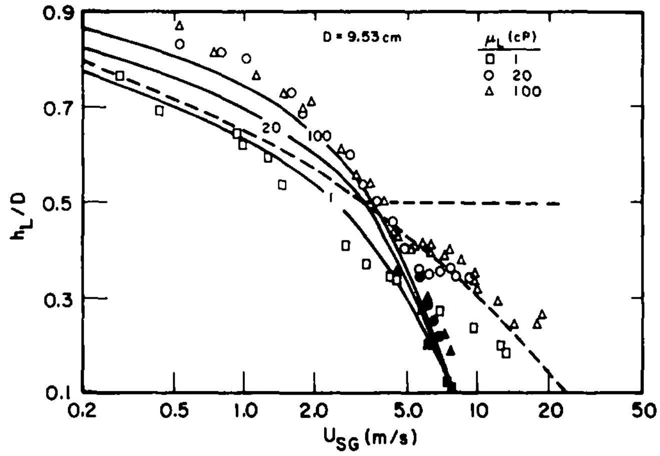

Figure 7. Initiation of slug flow or KH waves in the 9.53 cm pipe: - - -, Taitel & Dukler transitions; ——, approximate calculations of transitions to slugs (open symbols) or KH waves (solid symbols).

$h_L/D = 0.3$ large-amplitude waves appear on a 100 cP liquid at U_{SG} = ca. 6.5 m/s and slugs do not appear until U_{SG} = ca. 10 m/s.

For small h_L/D there is a transition from stratified-wavy flow to annular flow at large U_{SG}, rather than to slug flow. This is not shown in figure 7.

Figure 8 presents transition results for the 2.52 cm pipe. In this figure the initiation of slugging or of large-amplitude waves are treated the same. No observations are presented of the initiation of slugs on a liquid interface that had large-amplitude waves present. The results shown in figure 8 thus represent either a transition to slugs or, for $U_{SG} > 4$ m/s, to a stratified flow with KH waves.

The important result to be noted in both figures 7 and 8 is that liquid viscosity has a stabilizing effect in that larger values of h_L/D are required for large viscosities. It is also noted that an asymptotic behavior is observed for viscosities >ca. 20 cP, whereby the transition is insensitive to changes in viscosity.

The results shown in figures 7 and 8 could help explain the observed effect of liquid viscosity on the initiation of slug flow discussed in the previous section. An increase in liquid viscosity

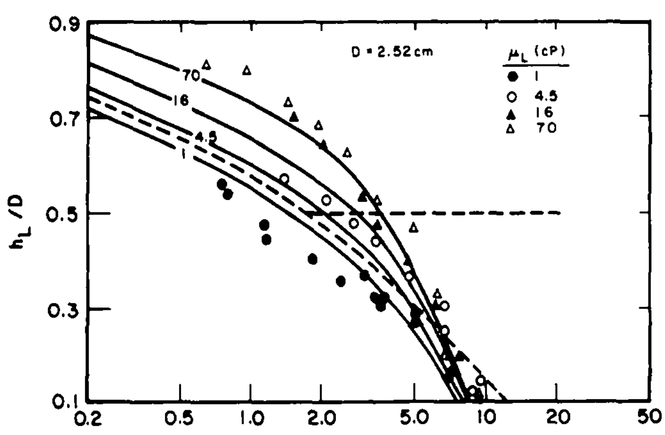

Figure 8. Initiation of slug flow or KH waves in the 2.5 cm pipe: - - -, Taitel & Dukler transitions; ——, approximate calculations of transitions to slugs (open symbols) or KH waves (solid symbols).

increases the h_L/D corresponding to a given U_{SL} and, because of this, tends to cause transition at lower U_{SL}. However, for viscosity changes from 1 to 20 cP this is counterbalanced by the stabilizing effect shown in figures 7 and 8. This explains the small effect on the U_{SL} required for transition caused by viscosity changes from 1 to 4.5 cP, shown in figure 2, and from 1 to 20 cP, shown in figure 3. However, figure 4 shows a large effect on the U_{SL} at transition for a viscosity change from 1 to 100 cP, because the destabilizing effect of increasing $h_L D$ outbalances the stabilizing effect from an increase in liquid viscosity, shown in figures 7 and 8.

(c) Visual observations

The first slugs for liquid viscosities <20 cP were always observed in the downstream half of the pipeline, despite the fact that h_L was larger in the upstream section. For the 100 cP liquid in the 9.53 cm pipe the first slug usually was observed slightly downstream of the entry, but frequently they were observed to be coming from the mixing section at the entry to the pipeline.

The mechanisms for the transition from a stratified flow to a slug flow for $U_{SG} < 4$ m/s is most clearly seen for runs with high viscosity liquids because the interface of the stratified flow is smooth. Consequently, special care was taken to avoid the formation of slugs at the entry where observations could not be made. This was done by elevating the entry from the rest of the pipe by about one-tenth of a pipe diameter. This caused the liquid height at the entry to be smaller than in the rest of the pipe. The first interfacial disturbances were then observed far downstream of the entry where h_L had a fairly constant value.

For runs with the highest viscosity liquids in both the 2.52 and 9.52 cm pipes, the first disturbances prior to the appearance of slugs were very small sinusoidal disturbances with a wavelength of 2–3 cm. These were present for a fraction of a second and quickly gave way to a large-amplitude wave which grew very rapidly to bridge the whole pipe. With increasing U_{SG} the liquid layer is thinner at the transition. Eventually, at sufficiently large U_{SG} the liquid layer is so thin that the large-amplitude, large-wavelength waves that emerge out of the regular disturbances are not able to grow to bridge the pipe cross section. Instead they are the irregular waves, identified by Francis and by Andritsos & Hanratty, which cause larger increases in the interfacial stress and a thinning of the liquid layer.

For intermediate liquid viscosities and for gas velocities <3 m/s, the first slugs appeared close to the midsection of the pipe by the following mechanism. When the liquid was thick enough for the appearance of slugs, a short length of the liquid was covered with small sinusoidal disturbances. These persisted for a few seconds before producing a large-amplitude wave which evolved into a slug after traveling a distance of about 1 m. At $U_{SG} = 3 - 4.5$ m/s the small-amplitude waves, which first appeared on the stratified liquid with increasing liquid flow, covered the whole length of the pipeline. With a slight increase in U_{SL} the small-amplitude waves changed to large-amplitude KH waves. One of these quickly evolved into a slug; ocassionally, a slug was produced by the coalescence of two waves. A slug, once formed, moved quickly down the pipe and thinned out the liquid layer before another could appear.

Figure 9a is a photograph of regular 2-D waves which covered the whole length of the pipe, where the direction of flow is from right to left. If the liquid is then enough these regular waves can evolve into irregular large-amplitude waves such as shown in figure 9(f). Figures 9(d, e) show the front and tail of a large-amplitude wave which has just grown to form a slug on a thick liquid layer. Figures 9(b, c) show the front and back of a slug that was formed 80 pipe diameters upstream from where the photograph was taken.

The first slugs that are formed act as a "sweep" by taking fluid in at the front to increase in size and leaving a thin liquid layer behind. As shown in figures 9(d, e) there is a dip in the film thickness behind the slug. As shown in figure 10, the slug velocity at large gas velocity, measured as the time for the slug to move the distance between the two parallel-wire conductance probes, is approximately equal to the actual gas velocity just behind the slug. At low gas velocities, for which there are large hydraulic gradients in the pipe, the slug velocity appears to be greater than the gas velocity at the downstream location at which wave velocity measurements were made.

For conditions under which at most one slug existed in the pipe, the exit of a slug from the pipe resulted in a pressure release, even at low gas velocities. The gas acceleration that resulted from this pressure release instantaneously triggered the formation of regular sinusoidal surface disturbances. If the film thicknesses was high enough, a second and, sometimes, a third slug were formed. These "satellites" moved at lower velocities than the original slug because of the lower liquid levels in front and behind the "satellite".

For $U_{SG} > 4.5$ m/s KH waves are present on the liquid layer prior to the initiation of slug flow. Lin & Hanratty (1987a) pointed out that, for these values of U_{SG}, slugs are formed by the coalescence of the large-amplitude waves. This process is very clearly seen in experiments with high viscosity liquids. At low liquid velocities the KH waves are observed to coalesce and accelerate and then break up and decelerate. However, at sufficiently large liquid flows (or sufficiently high liquid viscosities) these waves come together in a group and form a disturbance which grows to a sufficiently large height to cover the pipe cross section. Slugs formed in this way have a short length and are highly aerated. The film thickness in front and behind them are seen to be approximately he same, so they do not increase in size as they move down the pipe.

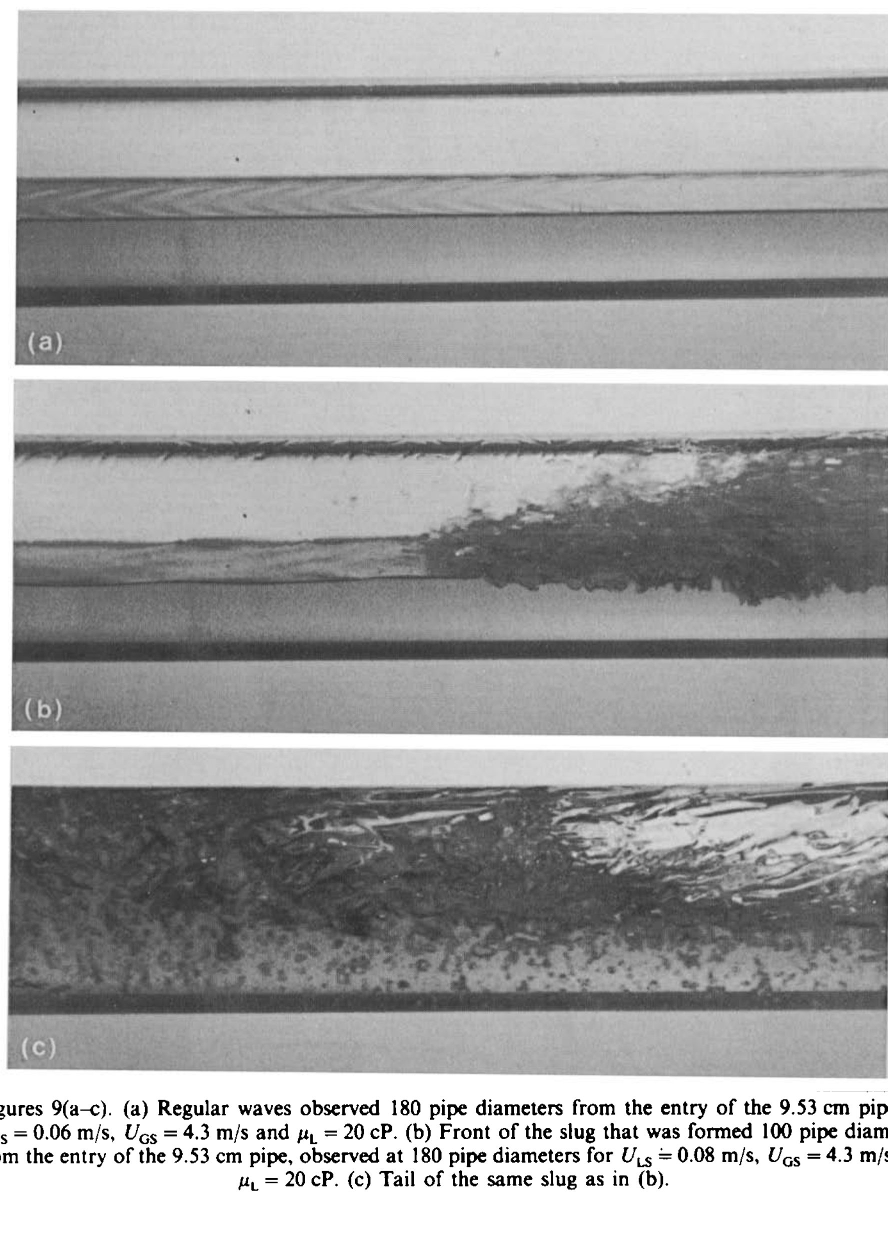

Figures 9(a–c). (a) Regular waves observed 180 pipe diameters from the entry of the 9.53 cm pipe for $U_{LS} = 0.06$ m/s, $U_{GS} = 4.3$ m/s and $\mu_L = 20$ cP. (b) Front of the slug that was formed 100 pipe diameters from the entry of the 9.53 cm pipe, observed at 180 pipe diameters for $U_{LS} = 0.08$ m/s, $U_{GS} = 4.3$ m/s and $\mu_L = 20$ cP. (c) Tail of the same slug as in (b).

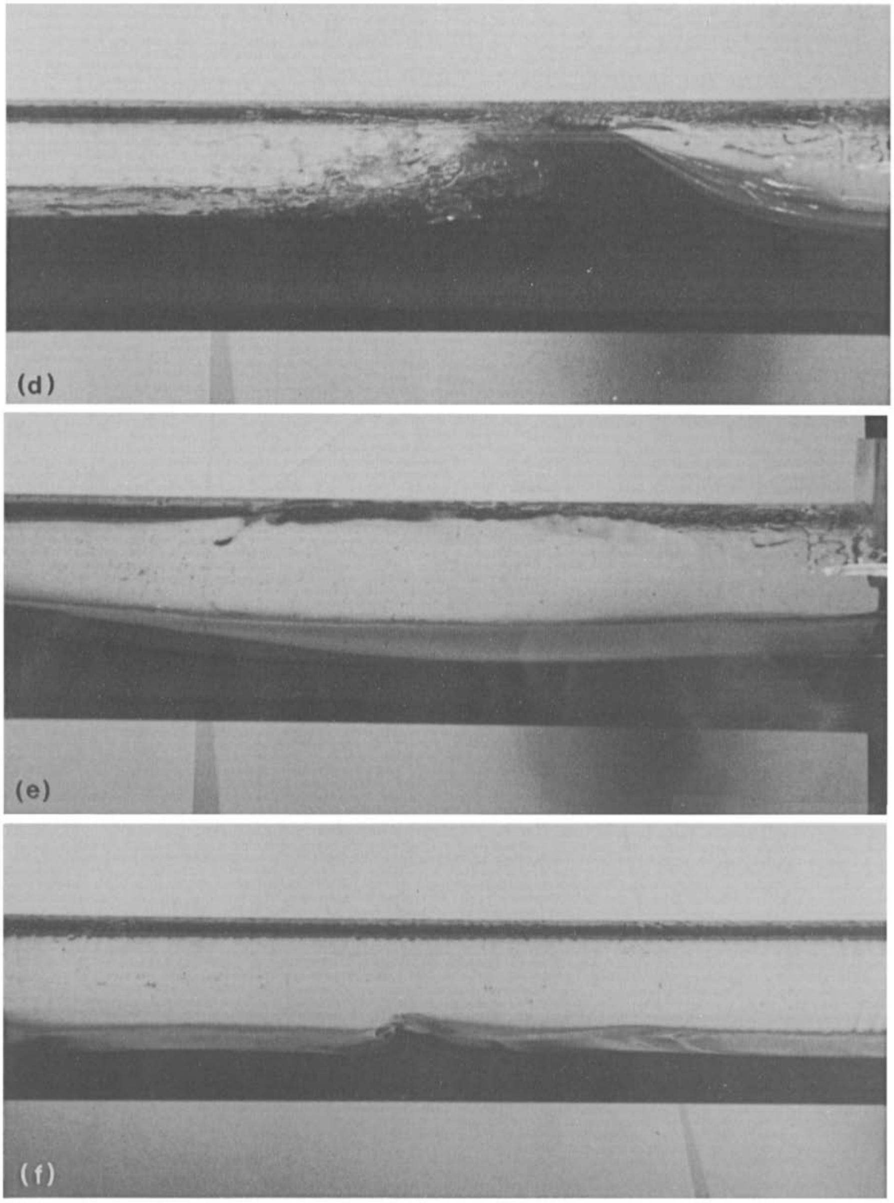

Figures 9(d–f). (d) Slug that has just been formed 30 pipe diameters from the entry of the 9.53 cm pipe for $U_{LS} = 0.033$ m/s, $U_{GS} = 4$ m/s and $\mu_L = 100$ cP. (e) Tail of the same slug as in (d). (f) Large-amplitude wave observed 30 pipe diameters from the entry of the 9.53 cm pipe for $U_{LS} = 0.033$ m/s, $U_{GS} = 7$ m/s and $\mu_L = 100$ cP.

DISCUSSION

(a) Comparison with previous analyses

The non-linear analyses that have been presented in the literature predict that a plot of h_L/D at the stratified–slug flow transition vs U_{SG}, for a given pipe diameter, should be independent of liquid viscosity. Figures 7 and 8 clearly are contradictory to this.

For example, the Taitel & Dukler (1976) analysis predicts the appearance of intermittent flow to the right of the dashed curve and above the horizontal dashed line. It predicts the appearance of annular flow beneath the horizontal dashed line. It is noted that the results for water at low U_{SG} are in good agreement with the analysis. However, the analysis underpredicts the h_L/D required for the initiation of slugs in high viscosity liquids.

The results in figures 7 and 8 would seem to support the large-wavelength viscous analysis of Lin & Hanratty (1986). See, for example, the calculations for a rectangular channel in figure 1.

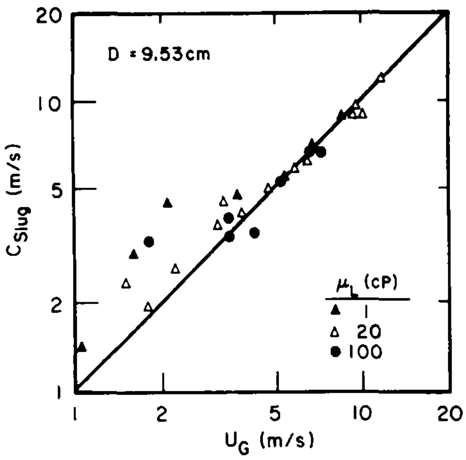

Figure 10. Slug velocity as a function of the gas velocity behind the slug.

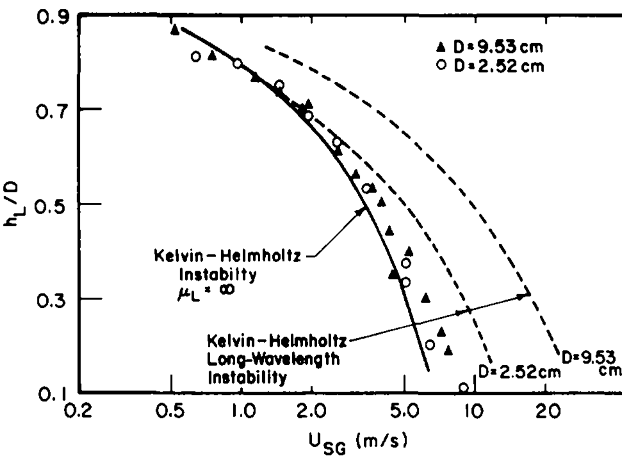

Figure 11. Comparison of KH stability calculations with the observed initiation of slugs or large-amplitude waves on a 70 cP (D = 2.52 cm) and a 100 cP (D = 953 cm) liquid.

However, a closer examination reveals discrepancies. This is particularly true for experiments in the 9.53 cm pipe with U_{SG} close to 3 m/s and experiments with high liquid viscosities.

(b) Experiments with high liquid viscosities

Figures 7 and 8 show that curves representing the transition to KH waves are continuous with the curves representing the transition to a slug flow. This result would seem to suggest that the same instability mechanism is responsible for both transitions.

Figure 11 is a plot of the high viscosity runs shown in figures 7 and 8. The striking feature of this plot is that the data for the two pipe diameters fall on the same curve. This is in contradiction to the analysis of Lin & Hanratty and Taitel & Dukler, which would predict h_L/D to be a function of the dimensionless group $[(U_{SG}/(gD)^{1/2}]\ [(\rho_G/\rho_L)^{1/2}]$.

The visual observations presented in the previous section shown that a precursor to the appearance of slugs or of KH waves on high viscosity liquids is an instability which leads to small-wavelength sinusoidal disturbances. This would seem to suggest that the assumption made by Lin & Hanratty that slugs at $U_{SG} < 4$ m/s are the result of the growth of an infinitesimal large-wavelength disturbance could be incorrect.

Therefore, stability calculations, which are not restricted to the assumption of large-wavelength waves, were carried out. Neutral stability curves obtained by using a completely inviscid analysis ([1] with h_G approximated as in [10] and [11]) are given in figures 12–14. Justifications for using an inviscid analysis are that Andritsos & Hanratty (1987a) have shown that this assumption gives results in approximate agreement with the observed critical gas velocity for the initiation of large-amplitude waves on relatively thin liquid layers and that Lin & Hanratty (1986) have found that the stability of stratified flows to long-wavelength disturbances is independent of viscosity for high viscosities.

All of these neutral stability curves show a critical U_{SG} which is approximately independent of pipe diameter. This critical condition corresponds to a wavelength in the neighborhood of 1.5–3.0 cm. It is also noted that the value of U_{SG} needed for the generation of large-wavelength waves (given by [4]) is larger than the critical U_{SG} and is strongly dependent on pipe diameter. For $h_L/D = 0.7$, the difference between the critical U_{SG} and the stability condition for large wavelengths is quite small. However, as h_L/D decreases the difference becomes significant and can be quite large for large diameter pipes.

The gas velocities at which slugs were first observed in the 2.52 and 9.53 cm pipes for high viscosity liquids are indicated at the bottom of graphs. It is noted that the initiation of slugs corresponds to the critical U_{SG} and not to the value predicted by [4]. For thin liquid layers ($h/D = 0.3$), it is seen that the critical U_{SG} corresponds to the initiation of KH waves. The agreement of this stability analysis with the observed appearance of slugs or KH waves is again shown in figure 11 where the curve represents the calculated critical U_{SG}. The dashed curves indicate

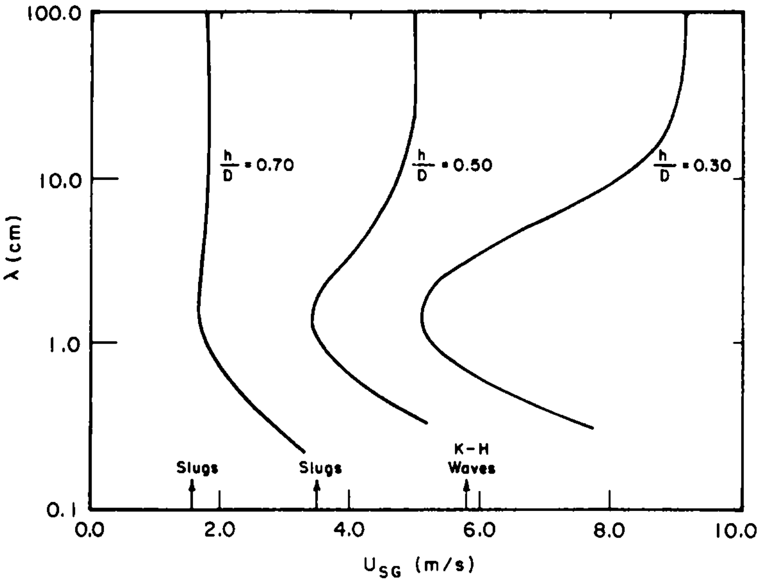

Figure 12. Neutral stability curves for the flow of air and a very viscous liquid ($\rho_L = 1.22$ g/cm^3, $\mu_L = \infty$) through a 2.52 cm pipe.

calculations based on [4]. These indicate that long-wavelength stability theory disagrees with experiments and predicts a strong effect of pipe diameter.

(c) Experiments with low liquid viscosities

The results of the experiments with the low viscosity liquids are different from those with the high viscosity liquids. As already shown by Lin & Hanratty, the U_{SG} required for the initiation of slugs is dependent on pipe diameter. Water transition results at $U_{SG} < 3$ m/s for both the 9.53 and 2.52 cm pipes come together on a single curve of h_L/D vs $[U_{SG}/(gD)^{1/2}][\rho_G/\rho_L)^{1/2}]$.

This different effect of pipe diameter for low and high viscosity liquids can be understood by considering the figure 12. Neutral stability diagrams for low viscosity liquids, that consider only the effect of pressure variations in phase with the wave height have a form, for $h_L/D \geqslant 0.4$, similar to that shown in figure 12 for high viscosity liquids for $h_L/D \geqslant 0.7$. The long-wavelength viscous solution, which is dependent on pipe diameter, would influence the calculated critical U_{SG}

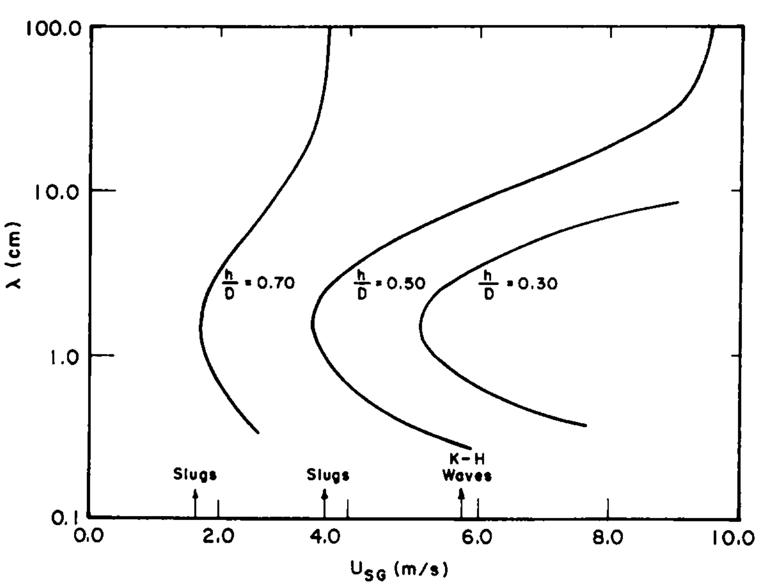

Figure 13. Neutral stability curves for the flow of air and a very viscous liquid ($\rho_L = 1.22$ g/cm^3, $\mu_L = \infty$) through a 9.53 cm pipe.

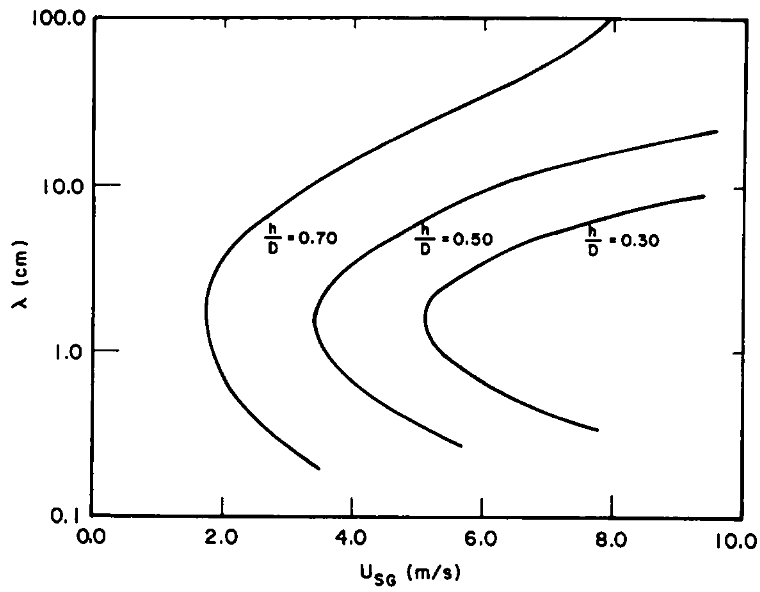

Figure 14. Neutral stability curves for the flow of air and a very viscous liquid ($\rho_L = 1.22$ g/cm^3, $\mu_L = \infty$) through a 50.8 cm pipe.

for air–water flows at $U_{SG} < 3$ m/s and, in fact, would be a good approximation for the critical U_{SG}.

APPROXIMATE CALCULATION OF THE TRANSITION

An exact stability calculation for a range of liquid viscosities from 1 to 100 cP is difficult because of the problem of obtaining a solution for the liquid-phase flow field which includes viscous effects for both large and small wavelengths, and for both laminar and turbulent flows. In order to present some preliminary general results an approximate approach has been taken.

Small-wavelength effects were taken into account in the gas-phase calculations, so as to represent accurately pressure variations at the interface. Viscous effects were taken into account by using the long-wavelength solution of Lin & Hanratty so as to capture the destabilizing effect at low liquid viscosities found by them.

The pressure amplitude term, $\hat{P}_i$, in the Lin & Hanratty analysis was therefore multiplied by the factor $k\bar{H}_G \coth(k\bar{H}_G)$, where k is the wavenumber and $\bar{H}_G$ is an equivalent gas height (Chow 1959), defined as

$$\bar{H}_G = A_G|S_i \qquad h_L/D \geqslant 0.5 \qquad [10]$$

and

$$\bar{H}_G = (0.5D - H_L) + \bar{H}_G|_{h_L:D=0.5} \qquad h_L/D < 0.5 \qquad [11]$$

In addition, the Ψ term defined by Lin & Hanratty to take account of the influence of liquid Reynolds number on the interfacial friction factor was set equal to zero to agree with the recent results of Andritsos & Hanratty (1987b). The liquid flows for 1 and 4.5 cP liquids in the 2.52 cm pipe and for 1 and 20 cP liquids in the 9.53 cm pipe were considered turbulent. A value of the friction factor ratio, f_i/f_S, equal to two was selected as a reasonable average representation of the interfacial stress for water.

Calculated transition curves for different liquid viscosities are plotted as the solid curves in figures 7 and 8. As has already been indicated in figure 11, the 70 cP curve for $D = 2.52$ cm and the 100 cP curve for $D = 9.53$ cm agree. The calculated curves for low viscosities show the strong effect of pipe diameter already discussed. This is illustrated in the calculations for a liquid viscosity of 1 cP shown in figure 15. Approximate agreement between the calculations and experimental results is shown in the figures, except that the experiments show no difference between the 16 and 70 cP liquids in the 2.52 cm pipe and between the 20 and 100 cP liquids in the 9.53 cm pipe.

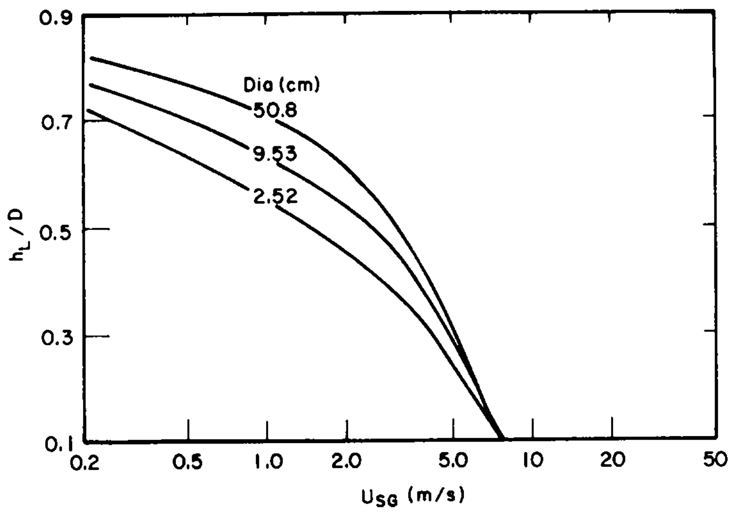

Figure 15. Calculated transitions to slug flow or KH waves for a 1 cP liquid.

The calculated results for a fully-developed flow are presented in a Mandhane plot in figure 16. There is qualitative agreement with the results presented in figures 2–4 and in figures 12–14 of the paper by Andritsos & Hanratty (1987a). An increase of viscosity from 1 to 4.5 cP for $D = 2.52$ cm and from 1 to 20 cP for $D = 9.53$ cm has a small effect because of the counterbalancing of the destabilization associated with the increase in h_L/D and the viscosity stabilization shown in figures 7 and 8. Further increases in viscosity are shown to cause a sharp decrease in the U_{SL} required for transition to an intermittent flow such as shown in figure 4. The detailed quantitative agreement between these calculations and measurements is not so good because in the experimental system the flow is not well-developed and because the model used to calculated U_{SL} for a fixed h_L/D and U_{SG} is not exact.

COMPARISON WITH OTHER MEASUREMENTS

Wu *et al.* (1987) recently studied gas–condensate flow in a horizontal 20.3 cm pipe at 75 b pressure. They reported transitions to slug flow at superficial liquid velocities in the range of 1 m/s for superficial gas velocities of 0.7–8 m/s. Comparisons should be made at the same value of $\rho_G^{1/2} U_{SG}$. Because of the high density of the gas, their tests should correspond to results in this paper

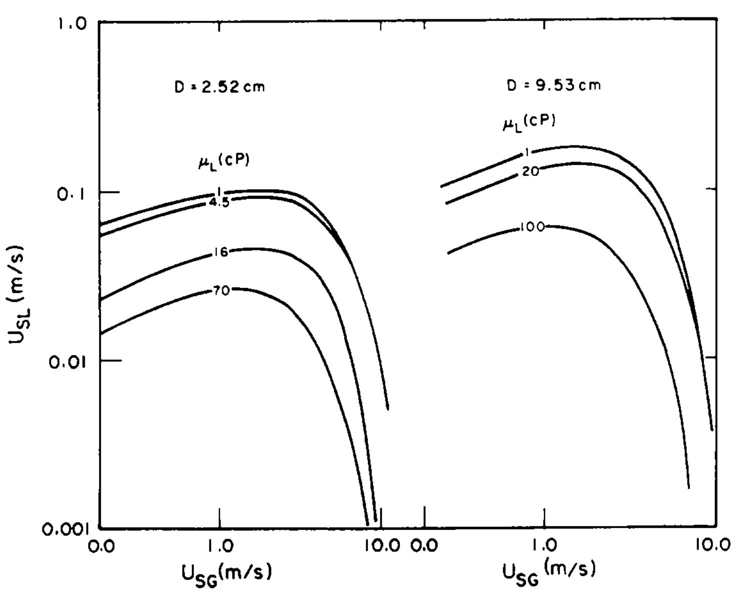

Figure 16. Calculated transitions to slug flow or KH waves presented in a Mandhane plot.

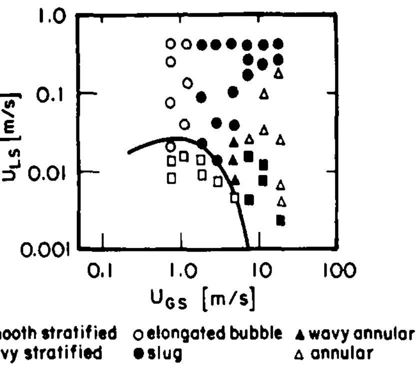

Figure 17. Flow patterns for a 90 cP glycerine/water and air mixture in a horizontal 3.8 cm pipe (Taitel & Dukler 1987).

in the region of $U_{SG} > 5$ m/s. It is quite probable that they were observing flows for which the mechanism for the generation of slugs is the coalescence of KH waves. If this is the case, then linear stability predicts the initiation of large-amplitude waves, but not slugs.

Figure 17 gives a comparison of the calculations outlined in the previous section with the measurements of Taitel & Dukler (1987), done in a 3.8 cm pipe with a liquid viscosity of 90 cP. Good agreement is noted both with the observed transitions to KH waves and to intermittent flow.

CONCLUDING REMARKS

A comparison of experimental results on the stability of a stratified flow is best done on a plot of h_L/D vs U_{SG} rather than with the Mandhane coordinates, U_{SL} vs U_{SG}. This is so, not only because an evaluation of theories is more easily done, but also because effects associated with a non-developed flow may be less important.

Experimental results on the effect of liquid viscosity on the initiation of slugs show a stabilization with increasing liquid viscosity in this type of plot, as predicted by Lin & Hanratty. This would seem to contradict interpretations which use a long-wavelength inviscid analysis.

Lin & Hanratty argued that at small U_{SG} the initiation of slugs occurs through the growth of long-wavelength infinitesimal disturbances. They showed that liquid inertia is destabilizing if viscous effects are included and that this effect decreases for fixed values of h_L/D and U_{SG}. For very large liquid viscosities where inertia is neither stablilizing nor destabilizing the Lin & Hanratty analysis gives the same results as a long-wavelength KH analysis.

At first glance the observed effect of liquid viscosity and the good agreement of experimental results for air–water with the prediction would seem to support the mechanism explored by Lin & Hanratty. However, a closer examination of the results with very viscous liquids shows a different effect of pipe diameter than is predicted.

Visual observations of the stability of a very viscous liquid show that the first waves that appear are sinusoidal and have a sufficiently short wavelength that they are affected both by gravity and surface tension. With a slight change in the flow conditions large-amplitude isolated disturbances grow out of these regular small-wavelength waves. If the liquid layer is thick enough the disturbances touch the top wall and form slugs. On the thin layers that occur for $U_{SG} > 4$ m/s these disturbances evolve into large-amplitude irregular waves that cause a large increase in the interfacial stress and a large decrease in the thickness of the liquid. At small liquid heights (or liquid flows) there is no tendency for these waves to coalesce. However, at some critical condition they group together to form a large disturbance that grows into a slug.

The evolution of the large-wavelength disturbances from the regular wave train occurs by non-linear processes which are not yet understood. However, if the appearance of the small-wavelength sinusoidal wave train is a necessary condition then linear theory still can be used to predict stability. Stability calculations that abandon the large-wavelength approximation support this suggestion in that the critical U_{SG} for the initiation of the small-wavelength waves due to gas-phase pressure variations in phase with the wave height is the same as the observed U_{SG} for the initiation of slugs or of large amplitude irregular waves.

Observations of the mechanism for the initiation of slugs for liquids with viscosities close to that of water is complicated because over a large range of flow conditions the interface of the stratified flow is covered with waves (generated by gas-phase pressure variations in phase with the wave slope) prior to the appearance of slugs. However, at very low gas velocities, where the interface is smooth, Lin (1985) has reported the same phenomena that were observed on very viscous liquids. This result, plus the agreement of experiments with the approximate calculations presented in this paper, would tentatively suggest that the type of mechanism observed for very viscous liquids could be operative for all viscosities.

Calculations with a more accurate representation of viscous effects in the liquid, than is used in the section on approximate calculations, are needed to clarify this question.

Acknowledgements—This work has been supported by the Shell Companies Foundation and by the Department of Energy under DOE DEFG02-86E R 13556.

REFERENCES

ANDREUSSI, P. & PERSEN, L. N. 1987 Stratified gas–liquid flow in downwardly inclined pipes. Private communication.

ANDRITSOS, N. 1986 Effect of pipe diameter and liquid viscosity on horizontal stratified flow. Ph.D. Thesis, Univ. of Illinois, Urbana.

ANDRITSOS, N. & HANRATTY, T. J. 1987a Interfacial instabilities for horizontal gas–liquid flows in pipelines. *Int. J. Multiphase Flow* **13,** 583–603.

ANDRITSOS, N. & HANRATTY, T. J. 1987b Influence of interfacial waves on hold-up and frictional pressure drop in stratified gas–liquid flows. *AIChE Jl* **33,** 444–454.

CHOW, V. T. 1959 *Open-channel Hydraulics*. McGraw-Hill, New York.

FRANCIS, J. R. D. 1954 Wave motions and the aerodynamic drag on a free oil surface. *Phil. Mag.* **45,** 695–702.

FRANCIS, J. R. D. 1956 Wave motions on a free oil surface. *Phil Mag.* **1,** 685–688.

HANRATTY, T. J. 1987 Gas–liquid flow in pipelines. *PhysicoChem. Hydrodynam.* **9,** 101–114.

KORDYBAN, E. S. 1977 Some characteristics of high waves in closed channels approaching Kelvin–Helmholtz instability. *ASME Jl Fluids Engng* **99,** 339–346.

KORDYBAN, E. S. & RANOV, T. 1970 Mechanism of slug formation in horizontal two-phase flow. *J. basic Engng* **92,** 857–864.

LIN, P. Y. 1985 Flow regime transitions in horizontal gas–liquid flow. Ph.D. Thesis, Univ. of Illinois, Urbana.

LIN, P. Y. & HANRATTY, T. J. 1986 Prediction of the initiation of slugs with linear stability theory. *Int. J. Multiphase Flow* **12,** 79–98.

LIN, P. Y. & HANRATTY, T. J. 1987a Effect of pipe diameter on the interfacial configurations for air–water flow in horizontal pipes. *Int. J. Multiphase Flow* **13,** 549–563.

LIN, P. Y. & HANRATTY, T. J. 1987b Detection of slug flow from pressure measurements. *Int. J. Multiphase Flow* **13,** 13–21.

MILES, J. W. 1959 On the generation of surface waves by shear flows. Part 3, Kelvin–Helmholtz instability. *J. Fluid Mech.* **6,** 583–598.

MISHIMA, K. & ISHII, M. 1980 Theoretical prediction of onset of horizontal slug flow. *Trans. ASME Jl Fluids Engng* **102,** 441–445.

TAITEL, Y. & DUKLER, A. E. 1976 A model for predicting flow regime transitions in horizontal and near horizontal gas–liquid flow. *AIChE Jl* **22,** 47–55.

TAITEL, Y. & DUKLER, A. E. 1987 Effect of pipe length on the transition boundaries for high-viscosity liquids. *Int. J. Multiphase Flow* **13,** 577–581.

WALLIS, G. B. & DOBSON, J. E. 1973 The onset of slugging in horizontal stratified air–water flow. *Int. J. Multiphase Flow* **1,** 173–193.

WU, H. L., POTS, B. F. M., HOLLENBERG, J. F. & MEERHOF, R. 1987 Flow pattern transitions in two-phase gas/condensation flow at high pressures in an 8-inch horizontal pipe. Presented at the *3rd Int. Conf. on Multiphase Flow*, The Hague, The Netherlands.